

Recent progress of multi-junction solar cell development for CPV applications at AZUR SPACE

Cite as: AIP Conference Proceedings **2149**, 020007 (2019); <https://doi.org/10.1063/1.5124177>
Published Online: 26 August 2019

Rosalinda H. van Leest, Daniel Fuhrmann, Alexander Frey, Matthias Meusel, Gerald Siefer, and S. Kasimir Reichmuth



View Online



Export Citation

ARTICLES YOU MAY BE INTERESTED IN

[Characterisation and impact of non-uniformity on multi-junction solar cells \(MJSC\) caused by concentrator optics](#)

AIP Conference Proceedings **2149**, 020004 (2019); <https://doi.org/10.1063/1.5124174>

[Challenges in the design of concentrator photovoltaic \(CPV\) modules to achieve highest efficiencies](#)

Applied Physics Reviews **5**, 041601 (2018); <https://doi.org/10.1063/1.5046752>

[FLATCON[®] CPV module technology: A new design based on the evaluation of 10 years of outdoor measurement data](#)

AIP Conference Proceedings **2149**, 030007 (2019); <https://doi.org/10.1063/1.5124184>

Lock-in Amplifiers
up to 600 MHz



Recent Progress of Multi-Junction Solar Cell Development for CPV Applications at AZUR SPACE

Rosalinda H. van Leest¹, Daniel Fuhrmann^{1, a)}, Alexander Frey¹, Matthias Meusel¹, Gerald Siefer² and S. Kasimir Reichmuth²

¹*AZUR SPACE Solar Power GmbH, Theresienstrasse, 2, 74072 Heilbronn, Germany*

²*Fraunhofer Institute for Solar Energy Systems ISE, Heidenhofstraße 2, 79110 Freiburg, Germany*

^{a)} Corresponding author: Daniel.Fuhrmann@azurspace.com

Abstract. The next generation concentrator photovoltaic (CPV) solar cell from AZUR SPACE will be a five-junction upright metamorphic (5J-UMM) cell that is currently under development. The main design criteria for this 5J-UMM cell is to allow for the highest possible system performance instead of the highest cell efficiency under concentrating standard test conditions (CSTC) while retaining a low €/W price on system level. Our new 4J-UMM space solar cell has been used as the basis for the 5J-CPV cell. In subsequent development steps, a fifth subcell was added to the 4J-UMM structure and the band gap for each subcell was optimized for the terrestrial spectrum and for operating conditions of the system of 90°C. Furthermore, the tunnel diodes and the material quality of each subcell has been optimized. With this approach a 5.2 x 5.2 mm² 5J cell with 41% efficiency at 589 suns (25°C, AM1.5d) has been achieved. We expect the in-system performance of the current 5J-UMM cell already to be better compared to the existing triple junction solar cell product 3C44. Due to a severe current-mismatch in the current 5J-cell an immediate improvement potential of 8% in short circuit current density (J_{sc}) is available for a properly current-matched cell. Such an increased J_{sc} results in devices with efficiencies > 44% at CSTC.

INTRODUCTION

During the last decade AZUR SPACE has continuously improved the performance of its CPV solar cells [1,2], which has led to the market introduction of 3C44C in 2014. This is a 44%-class Germanium-based triple-junction solar cell now widely used in various CPV systems. With the triple-junction technology of 3C44C reaching a high level of maturity and a strong market demand for cells with higher output power and cost reduction at system level, the need arises to create a CPV solar cell with higher efficiency at reasonable cost impact. A similar demand exists for the space market and has led to the recent introduction of AZURs 4G32C-Adv [3], which is a four-junction (4J) upright metamorphic (UMM) solar cell with an initial (beginning-of-life BOL) efficiency of 32% and an end-of-life (EOL) efficiency of 28.7% (AM0, 1367W/m², 1E15 e⁻/cm²).

Compared to other approaches, such as inverted metamorphic (IMM) growth and semiconductor bonding technology (SBT), that have already demonstrated CPV efficiencies > 45% [4,5], upright metamorphic growth offers the advantage that only one epitaxial growth run is required and no specialized, expensive processing techniques (substrate removal, transfer to carrier, semiconductor bonding) are needed. On the other hand metamorphic growth contains the risk that subcell material quality is lower, particularly for the quaternary Al-containing materials AlInGaAs and AlInGaP, which could affect the cell performance. Nevertheless, we successfully demonstrated with a 4J-UMM device for space applications containing two Al-containing subcells, that sufficient material quality can be obtained with UMM growth.

With the identification of UMM growth as the currently most cost competitive option, the question remains how many subcells will be implemented. Compared to the 4J device for space, adding a fifth junction offers significantly higher efficiency potential, but provides only minor technical challenges. Additionally, it offers a higher V_{oc} and lower

J_{sc} , which is particularly advantageous for CPV applications, since electrical outputs are typically hampered by resistance losses that are quadratically dependent on the current density.

Taking these considerations into account a five-junction (5J) upright metamorphic cell design was identified as the most promising successor to 3C44C. The target efficiency for this cell design is 46% under high concentration (500-1000x), with a V_{oc} target of 5.52 V and a J_{sc} target of 9.4 A/cm² at 1000x, all at concentrating standard testing conditions (CSTC: 25°C, AM1.5d). In addition to these verifiable targets at CSTC, a further requirement was added to design for optimum performance at operation conditions. This means that a band gap combination (at 25°C) need to be chosen that has none of the subcell band gaps shift into (water) absorption bands in the terrestrial spectrum at operational temperatures up to 90°C in order to guarantee a stable J_{sc} under operation conditions. Ideally a final development step will include subcell current-matching in such a way that losses due to optical elements are minimized and differences of typical spectra for CPV locations compared to AM1.5d are accounted for.

APPROACH

The Ge/InGaAs/AlInGaAs/AlInGaP 4J-UMM cell designed for space applications (4G32C) was used as a basis for the development of the 5-junction UMM cell for CPV applications. In a first step a fifth InGaP subcell was implemented between the AlInGaAs and AlInGaP subcells in order to create a five-junction device. While the optimum bandgap combinations for CPV applications are different from the ones for space due to the presence of atmospheric effects, a bandgap optimization for the AM1.5d spectrum was carried out as a second step. For this bandgap optimization, the special requirement was added that the subcell bandgaps of J3 and J4 should not shift into the relevant water absorption bands in the AM1.5d spectrum at operation temperatures up to 90°C. Therefore quantum efficiency measurements were carried out at 25°C and 65°C for the first batch of 5J devices in order to determine temperature coefficients for the different subcell materials. These measurements were repeated for the second batch of 5J devices in order to check the optimized bandgap combination. After fixation of the band gaps, the tunnel diodes and subcells were optimized. For the tunnel diodes this included making sure the tunnel diodes can cope with concentration factors > 1000 suns (both before and after thermal load, caused by growth of subsequent solar cell layers) and developing a more transparent tunnel diode for application between the AlInGaP and InGaP subcells. Different growth conditions were tested in order to find the conditions that result in maximum material quality of the different subcells. These optimizations were implemented into a third batch of 5J devices. In a final iteration (still to be prepared) the subcell thicknesses will be optimized to create a current matched 5J device with a projected efficiency > 44% under concentration standard testing conditions (CSTC: 25°C, AM1.5d). EQE and IV measurements (both at 1 sun and under concentrated light) were performed in the CalLab of Fraunhofer ISE.

RESULTS

Figure 1a shows the external quantum efficiency (EQE) of a 4J-UMM structure developed for space applications where a fifth InGaP subcell has been implemented as J2. For reference purposes the AM1.5d reference spectrum is plotted in grey in the background. From these measurement it becomes clear that at 25°C the bandgap of the InGaAs J4 lies within one of the water absorption bands and the bandgap of the AlInGaAs J3 lies at the band edge of another water absorption band. Since CPV cells typically operate at much higher temperatures (up to approximately 90°C) this means that under real operation conditions the J3 bandgap will shift into an absorption band and the J4 will shift out of the absorption band. This will lead to a situation where current matching between the subcells is strongly dependent on the operation temperature, which change during the day. In order to avoid such shifts in current matching a second set of quantum efficiency measurements was made at 65°C (not shown here).

The V_{oc} , FF and efficiency of a first iteration 5J cell is plotted versus concentration factor x in figure 1b. A maximum efficiency of 38.4% is reached at 390 suns and the efficiency is greater than 38% in a broad concentration range from approximately 200 to 1000x. The subcell currents in figure 1a show that the cell is significantly current mismatched. Nevertheless, the data within figure 1 show that the 4J-UMM structure with additional InGaP subcell is already operational under CPV conditions and hence represents an excellent basis for our further development.

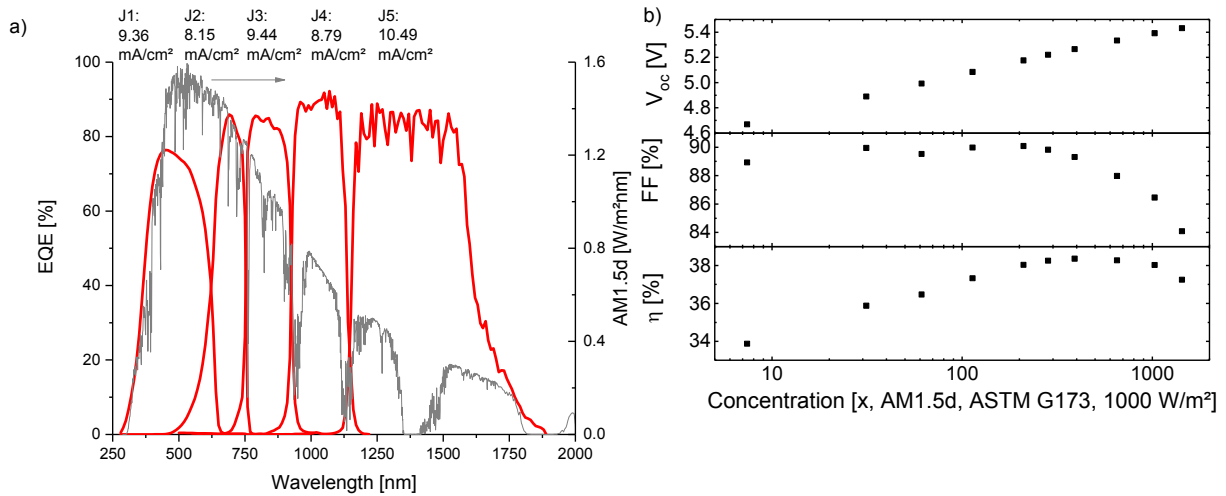


FIGURE 1. External Quantum Efficiency (EQE) of a first iteration of 5J-UMM cells, plotted together with the AM1.5d reference spectrum, subcell current densities (J_{sc}) indicated (a) and open circuit voltage (V_{oc}), Fill Factor (FF) and efficiency (η) plotted versus concentration factor (X) for the same cell (b).

Figure 2a shows the EQE of 5J cells with a bandgap combination optimized for operation temperatures up to 90°C (plotted in blue) in comparison to 5J-UMM cells of the first iteration (plotted in red) together with the AM1.5d spectrum in grey. It is clearly visible that at the measurement temperature of 25°C the band gaps of J3 and J4 are now no longer within or at the edges of the water absorption bands. Again a second set of EQE measurements was made at 65°C (not shown here) and from the 25 and 65°C measurements new temperature coefficients for the subcell materials were calculated. With these temperature coefficients the EQE for an operation temperature of 90°C was simulated. This simulated EQE for 90°C is plotted together with the measured EQE at 25°C and the AM1.5d reference spectrum for the J3 subcell and for the J4 subcell in figure 2b and figure 2c, respectively. From these simulated subcell EQEs it can be seen that at 90°C the band edge of the J3 subcell is well below the water absorption band edge between 925 and 975 nm, whereas the J4 band gap is exactly at the absorption band edge around 1115 nm. This shows that for operational temperatures up to 90°C the short circuit current density J_{sc} for a properly current-matched device will be relatively insensitive to operational temperature.

In figure 3 the V_{oc} , FF and efficiency for one of the 5J cells from the second batch are plotted versus concentration ratio. A maximum efficiency of 41.2% is reached at 486 suns and the efficiency is > 40.5% in a broad concentration range (approximately 200-1000x). The subcell currents in figure 2a show that the current matching between the subcells is much better compared to the previous batch. However, the 1000 suns V_{oc} of 5.47 V is still approximately 50 mV below the target of 5.52 V that shows that the material quality still needs to be improved.

After establishing a basic 5J-cell design with appropriate band gaps, the individual components (tunnel diodes and subcells) were investigated in more detail. For the tunnel diodes (TDs) special test structures were prepared. In a first step, the standard UMM tunnel diode that has been developed for 1 sun space applications, has been evaluated. It turned out that the minimum peak current density J_{peak} of the UMM tunnel diode already equals 39,000 suns at 10 mA/cm² as 1 sun J_{sc} . Additionally we could also prove the good thermal stability of the tunnel diode upon thermal load, which is important especially for the tunnel diodes between J4 and J5 or between J3 and J4 due to the longer epitaxial growth on top of those tunnel diodes within the 5J-cell.

Nevertheless, the standard UMM tunnel diode absorbs in the J2 wavelength range of the 5J-cell and reduces the J2 subcell current density significantly. Therefore a new transparent metamorphic tunnel diode has also been developed. Even though it shows a ~10x lower J_{peak} compared to the standard UMM tunnel diode, the minimum J_{peak} equals 3,000 suns at 10 mA/cm² as 1 sun J_{sc} without any additional resistance related voltage loss, which demonstrates that this tunnel diode is already usable for CPV applications. From EQE measurements on cells with the standard UMM TD and the more transparent TD between J1 and J2 (not shown here), it was estimated that J_{sc} will increase by 2% for a properly current matched 5J cell, if the more transparent tunnel diode is applied. Further improvements of the transparent tunnel diode are ongoing.

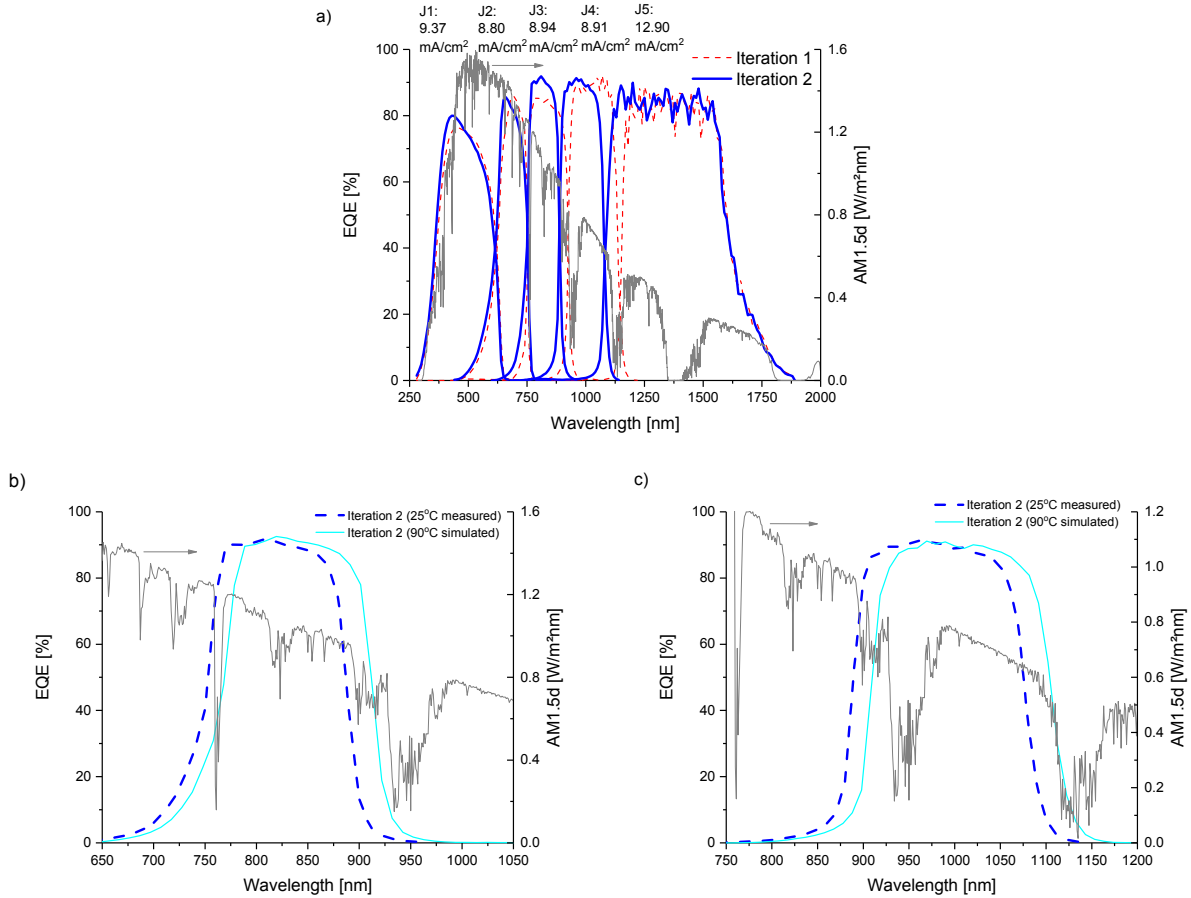


FIGURE 2. External Quantum Efficiency (EQE) of a second iteration 5J-UMM cell, plotted together with the EQE of a first iteration 5J-UMM cell and the AM1.5d reference spectrum, subcell current densities (J_{sc}) indicated (a). The measured EQE at 25°C and the simulated EQE at 90°C of a second Iteration 5J-UMM cell plotted together with the AM1.5d reference spectrum for the spectral region of the J3 (b) and spectral region of the J4 (c).

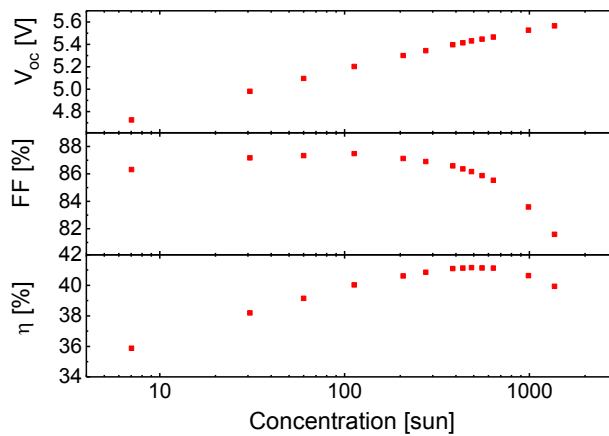


FIGURE 3. Open circuit voltage (V_{oc}), Fill Factor (FF) and efficiency (η) plotted versus concentration factor (X) of a second iteration 5J-UMM cell.

In addition to the tunnel diode optimization, the growth conditions of the individual subcells were optimized. In figure 4 the median measured V_{oc} (at 1 sun) of J1, J2, J3 and J4 isotypes is plotted versus the bandgap energy (E_{gap}). A reference line displaying the radiative limit is also plotted. The V_{oc} of the J4 isotypes is approximately 90 mV below the radiative limit and the V_{oc} of the J2 isotypes is approximately 115 mV below the radiative limit. This is significantly lower as compared to the Al-containing isotypes of J3 and J1, which exhibit a 150 mV and 180 mV lower V_{oc} compared to the radiative limit, respectively. Hence, particularly for the Al-containing subcells, a significant improvement potential regarding the material quality for 1 sun applications still exist.

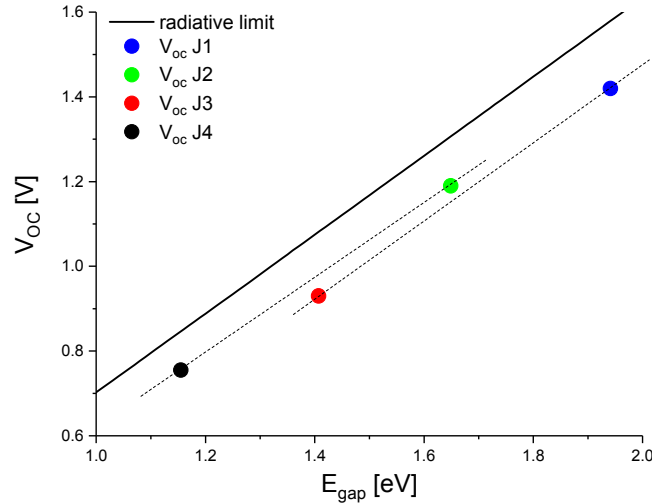


FIGURE 4. Median V_{oc} of J1 (blue), J2 (green), J3 (red) and J4 (black) isotype cells plotted versus bandgap energy E_{gap} . The black line represents the radiative limit whereas the dotted lines are guide for the eye.

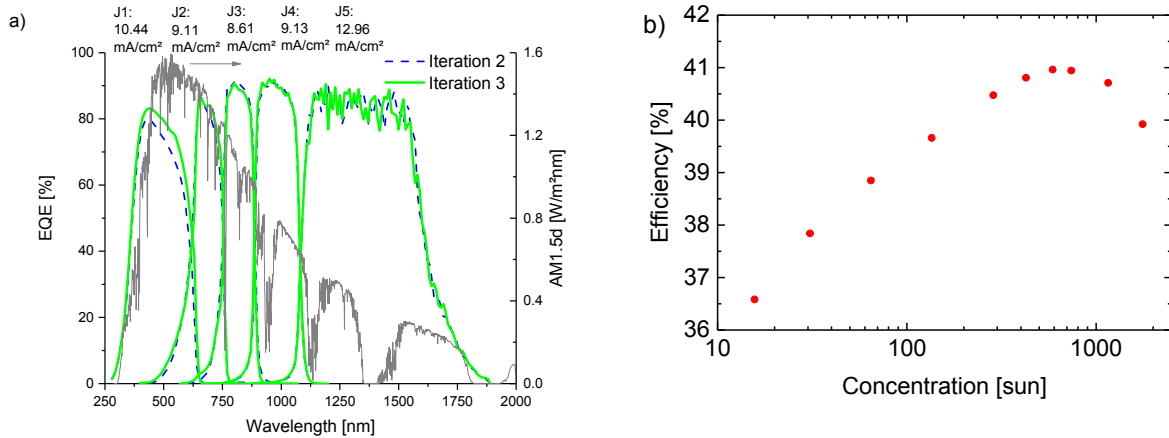


FIGURE 5. External Quantum Efficiency (EQE) of a third iteration 5J-UMM cell (bold, green), plotted together with the EQE of the second iteration (thin, blue) and AM1.5d reference spectrum (grey), subcell current densities (J_{sc}) indicated (a). Efficiency (η) plotted versus concentration factor (X) for the same cell (b).

With the optimized tunnel diodes and subcell materials, a new batch of 5J cells was prepared. At 1000 suns, the V_{oc} reaches a value of 5.52 V, which is 50 mV higher compared to the 2nd iteration of 5J-cells and already slightly above our initial V_{oc} -target. Due to the fact that the bandgap energy of each subcell of the 2nd and 3rd iteration of 5J-cells was almost identical (see figure 5a), this can be solely attributed to an improvement regarding the minority carrier lifetime of each subcell material. In addition, we can conclude that despite the improvement potential identified for 1 sun applications, the material quality is already suitable for CPV applications.

The EQE data of one of those cells is shown in figure 5a. Besides the EQE of the second batch and the AM1.5d spectrum are plotted for reference purposes as well. From these data, it is clear that the subcell current density in J1 is significantly increased, most likely due to a significantly improved minority carrier diffusion length compared to the previous batch of cells. The subcell currents of J2 and J4 have also increased slightly, whereas the J3 current density is slightly decreased and now the limiting subcell. Overall, the sum of the current densities for all subcells has been increased of about 1.3 mA/cm² for the third iteration of 5J-cells.

In figure 5b the efficiency of this 5J cell is plotted versus concentration factor and shows a maximum of 41% at 589x and efficiencies > 40.5% in a broad concentration range of approximately 300-1150x. This slightly reduced maximum efficiency shows the importance of current matching, which is planned for the next batch of 5J cells. Averaging the subcell currents of J1 to J4 results in a potential J_{sc} of 9.32 mA/cm², which represents an 8% increase compared to the 8.61 mA/cm² of the current 5J device. Assuming that the projected 8% J_{sc} increase also results in an 8% increase in efficiency, an efficiency of > 44% could be achieved for a properly current matched cell with the current material quality.

SUMMARY & OUTLOOK

A 5-junction upright metamorphic (5J-UMM) cell for CPV applications is currently under development at AZUR SPACE. In addition to a target efficiency of 46% at 500-1000x under concentrating standard test conditions (CSTC), the cell design will also be optimized for maximum in-system performance. Starting from a 4J-UMM cell developed for 1 sun space applications and after the implementation of a fifth subcell, a bandgap optimization for the terrestrial spectrum and an optimization of the tunnel diodes and the subcell materials took place. These results are already very close to the performance (in the lab) of a 3C44 cell with the same grid and dimensions. Due to the better adaption to operating conditions, the current 5J device is already expected to show better in system performance, despite the significant current-mismatch. In a next step the epitaxial structure will be optimized to realize current-matching between the subcells, which together with further improvements of the tunnel diodes and subcells, is expected to result in > 6%_{rel} higher system efficiencies. Additionally first module and reliability tests with 5J-cells are in preparation, which will also lead to a direct comparison between 3C44C and current 5J-devices regarding in-system performance.

ACKNOWLEDGEMENTS

This work was supported in part by the German Federal Ministry for Economic Affairs and Energy (BMWi) under the project QuintUMM (Contract number 0324152).

REFERENCES

1. D. Fuhrmann et al., "About 42%-class CPV cells and pathways beyond" Proc. of 9th International Conference on Concentrator Photovoltaics, Miyazaki, 2013.
2. V. Khorenko et al., "Roadmap for the next generations of European Space Solar Cells" 29th EU PVSEC, Amsterdam 2014.
3. T. Torunski et al., "Development and Qualification of Upright Metamorphic 4J Space Solar Cells4G32C-Advanced", Space Power Workshop, Torrance, CA, US, 2019.
4. J. Geisz et al., "50% or Bust: Status of Six-Junction Concentrator Solar Cells", CPV-15, Fes, Morocco, 2019.
5. F. Dimroth et al., "Four-junction wafer-bonded concentrator solar cells", *IEEE Journal of Photovoltaics* 6 (2016), No.1, pp.343-349